Nuclear Instruments and Methods in Physics Research B 315 (2013) 99–104

Contents lists available at SciVerse ScienceDirect

Nuclear Instruments and Methods in Physics Research B

journal homepage: www.elsevier.com/locate/nimb

Fragmentation ^{56}Fe on C, Al and CH_2 targets at 471 A MeV

Dong-Hai Zhang [a,*], Li-Chun Wang [b], Yan-Jing Li [b], Jun-Sheng Li [a], S. Kodaira [c], N. Yasuda [c]

[a] Institute of Modern Physics, Shanxi Normal University, Linfen 041004, China
[b] College of Nuclear Science and Technology, Beijing Normal University, Beijing 100875, China
[c] Fundamental Technology Center, National Institute of Radiological Science, 4-9-1 Anagawa, Inage-ku, Chiba 263-8555, Japan

ARTICLE INFO

Article history:
Received 15 October 2012
Received in revised form 23 May 2013
Accepted 31 May 2013
Available online 4 July 2013

Keywords:
Nuclear fragmentation
Angular distribution
Transverse momentum distribution
Temperature
CR-39

ABSTRACT

The emission angle and the transverse momentum distributions of projectile fragments (PFs) produced in fragmentation of ^{56}Fe on CH_2, C, and Al targets at 471 A MeV are measured. It is found that the angular and transverse momentum distribution of all PFs do not evidently depend on the mass of target nucleus, the average value and width of angular distribution decrease with increase of the charge of PF for the same target, and no obvious dependence of angular distribution on the mass of target nucleus is found for the same PF. The transverse momentum distribution of PF can be explained by a single Gaussian distribution and the averaged transverse momentum decreases with the increase of the charge of PF. The cumulated squared transverse momentum distribution of PF can be well explained by a single Rayleigh distribution. The temperature parameter of PF emission source decreases with the increase of the size of PF.

1. Introduction

Fragmentation, the breakup of a nucleus into a number of fragments in a wide range of masses, is a characteristic response of a highly excited nucleus. The knowledge of heavy ion fragmentation at intermediate and high energy (a few hundreds of MeV/nucleon) is important in nuclear physics, astrophysics, and health physics. For example, considering the biological effects of space radiation, when astronauts' mission is outside the earth magnetic field, they are exposed to Galactic Cosmic Radiation (GCR) and solar particle events, *e.g.*, showers of energetic charged particles from the surface of the Sun. These energetic charged particles would be the dominant source of the radiation dose and affect the health of humans on long-duration spaceflight both inside and outside the station. According to the GCR model developed by Badhwar and O'Neill [1], in unshielded free space in the inner heliosphere, iron ions deliver about 8% of the total dose from the GCR and 27% of the dose equivalent at times near solar maximum, even though they contribute less than 1% of the total GCR flux. So, the fragmentation of iron ions has been considerable interest in understanding their transport through matter and their biological effects.

At high energy (more than 1 GeV/nucleon) a large number of nuclear interactions occur producing a cascade of other ions and particles, building spectra of particles which are transported along the path of the initial ion. It has become clear that heavy ions have the largest radiological effects. In addition, the experimental results have revealed that the PFs are emitted with angles larger than the scattering angles of the beam, which further increases the spread of the beam. So far only a few measurements have been performed to analyze PFs emission angles for heavy ion collisions below 500 A MeV [2–4].

The fragmentation properties of ^{56}Fe on various targets at different energies have been studied by many groups [5–17], all of these studies are devoted to the total charge-changing cross sections and the partial cross sections of PFs productions.

In this paper we present the results of the emission angular distribution, transverse momentum distribution and the temperature of emission source of PF produced in fragmentation of 471 A MeV ^{56}Fe on C, Al, and CH_2 targets.

2. Experimental details

Stacks of C, Al and CH_2 targets sandwiched with CR-39 detectors were exposed normally to 471 A MeV ^{56}Fe beams at the Heavy Ion Medical Accelerator in Chiba (HIMAC) at the Japanese National Institute of Radiological Sciences (NIRS). A CR-39 sheet, about 0.77 mm in thickness, is placed before and after the targets. The thickness of carbon, aluminum and polyethylene targets is 5, 3, and 10 mm, respectively.

After exposure, the CR-39 detectors are etched in 7 N NaOH aqueous solution at temperature of 70 °C for 15 h. Tracks from beam ions and their fragments manifest in the CR-39 as etch-pit cones on both sides of CR-39 sheets. The images of ion tracks are scanned and analyzed automatically by HSP-1000 microscope system and the PitFit track measurement software [18], then checked

* Corresponding author. Tel./fax: +86 3572051347.
E-mail address: zhangdh@dns.sxnu.edu.cn (D.-H. Zhang).

0168-583X/$ - see front matter © 2013 Elsevier B.V. All rights reserved.
http://dx.doi.org/10.1016/j.nimb.2013.05.071

manually. The PitFit software provide some geometric information, such as the position coordinates, major and minor axes and area of etched track spot on CR-39 surfaces. About 2×10^4 Fe ions are traced from the first CR-39 detector surface in the stack. ^{56}Fe trajectories and the ones of secondary PFs are reconstructed in the whole stack. Details of track tracing and reconstruction, identification of charge of PFs can be found in our recent publication [19]. Because of the sensitivity of CR-39 detector, the tracks of PFs with charge $1 \leqslant Z \leqslant 5$ are not fully etched as a measurable spot. The emission angle θ of each PF is the angle of two simulated straight lines, *i.e.*, the straight line of primary iron ion track and the straight line of PF track. The straight line of primary iron ion track can be simulated by taking readings of the coordinates of the track on the entrance and the exit of the CR-39 detector surfaces before the target, and the straight line of PF track can be simulated by taking readings of the coordinates of the track on the entrance and the exit of the CR-39 detector surfaces after the target. The thickness of the CR-39 detector play an important role in the determination of the simulated straight line of primary iron ion track and PF track. The interaction point is in the target which can not be detected by the CR-39 detector.

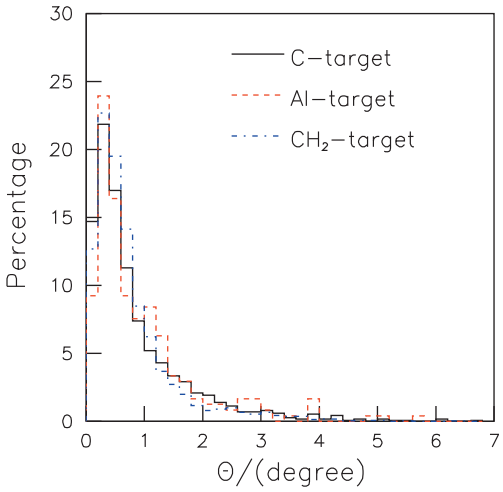

Fig. 1. The measured angular distribution of PFs with charge $Z \geqslant 6$ produced from the fragmentation of ^{56}Fe on different targets, the number of events for ^{56}Fe on C, Al, and CH_2 targets are 1135, 238, and 2206, respectively.

3. Results and discussion

Emission angular distribution and transverse momentum distribution of PFs provide information on the nuclear structure and on the mechanism of nuclear interaction by which fragments are produced. These distributions are also important in designing experiments with radioactive nuclear beams.

3.1. Angular distribution

Emission angle of each PF and scattering angle of iron ion are calculated from the coordinates of track positions on the top and bottom surfaces of CR-39 sheet after the target. The angular uncertainty is determined using the quadruplet fitting method [2]

$$\sigma(\theta) = \frac{\sqrt{\sigma_z^2 \sin^2\theta + 2\sigma_p^2 \cos^2\theta}}{2h}, \quad (1)$$

where σ_p is the positional uncertainty in x–y plane of the stack coordinate system which is about 3 μm, σ_z is the positional uncertainty in the z-axis which comes from stack composition and detector thickness measurement and is estimated at ≈8 μm for C-target, θ represents the emission angle. With a detector thickness of $h \approx 780$ μm we thus obtain angular uncertainty $\sigma(\theta) \approx 0.16^\circ$ for values of θ up to 8°.

Fig. 1 shows the angular distribution of the PFs for different targets. Most of PFs have the emission angle smaller than 1.5°, but some of PFs have emission angle as large as 8°. The angular distribution of all PFs does not depend on the mass of target nucleus.

Fig. 2 shows the emission angle distribution of PF with charge $Z = 6$, 18, 24 and 25 produced from the fragmentation of ^{56}Fe on C, Al and CH_2 targets respectively, the error bars shown in the figure are the statistical ones. For C target the average emission angle of PF with charge $Z = 6$, 18, 24 and 25 are 2.41 ± 0.20, 0.75 ± 0.06, 0.39 ± 0.02 and 0.29 ± 0.01 respectively. For CH_2 target the average emission angle of PF with charge $Z = 6$, 18, 24 and 25 are 2.24 ± 0.16, 0.71 ± 0.04, 0.44 ± 0.02 and 0.37 ± 0.01 respectively. For Al target the average emission angle of PF with charge $Z = 6$, 18, 24 and 25 are 3.08 ± 0.38, 1.05 ± 0.20, 0.35 ± 0.04 and 0.29 ± 0.02 respectively. From the figure it is shown that for the same target the average value and the width of the angular distribution decrease with increasing charge of PF, and for the same PF the average value and the width of the distribution do not evidently depend on the mass of target nucleus.

3.2. Transverse momentum distribution

The transverse momentum per nucleon (p_t) of a PF was calculated on the basis of its emission angle θ,

$$p_t = p \sin\theta, \quad (2)$$

where p is the momentum per nucleon of beam which can be calculated from beam energy per nucleon (E), $p = (E^2 + 2m_0E)^{1/2}$. m_0 is the nucleon rest mass and θ the emission angle of PF with respect to the beam direction.

Fig. 3 shows the transverse momentum distribution of PF with charge $Z = 6$, 18, and 24 produced from the fragmentation of ^{56}Fe on C and CH_2 targets, the error bars shown in the figure are the statistical ones. The distribution is fitted by a single Gaussian distribution. These Gaussians are in good agreement with prediction of the statistical model of Goldhaber [21]. This model assumes that the Fermi momenta of the nucleons in a fragment are statistically distributed as those in the original projectile nucleus. The averaged transverse momentum for PF with charge $Z = 6$, 18, and 24 are 44.23 ± 3.61, 13.80 ± 1.17, and 7.19 ± 0.41 A MeV/c, respectively, for C target, and 41.03 ± 2.86, 12.97 ± 0.69, and 8.08 ± 0.27 A MeV/c, respectively, for CH_2 target. For the same target the averaged transverse momentum and the width of the distribution increase with the decrease of the charge of PF. Projectile fragments come from the directly produced fragments (primary fragments) and the sequential decay fragments from excited primary fragment. The momentum distributions of the primary fragments are Gaussian distributions which are in good agreement with predictions of the statistical model of Goldhaber [21] and the momentum widths are basically related to initial Fermi momenta in the projectile. However, since the primary fragments are excited, they are deexcited by light particle evaporation. This secondary decay decreases the observed masses and increase the observed momentum widths of the primary fragments [22]. The contribution from sequential decay of primary fragments to the light projectile fragments are more important than that to the heavy projectile fragments, the widths of the transverse momentum distributions of light projectile fragments are greater than that of the heavy projectile fragments.